ACS APPLIED MATERIALS & INTERFACES

Research Article

www.acsami.org

Bio-Conjugated CNT-Bridged 3D Porous Graphene Oxide Membrane for Highly Efficient Disinfection of Pathogenic Bacteria and Removal of Toxic Metals from Water

Bhanu Priya Viraka Nellore,[†] Rajashekhar Kanchanapally,[†] Francisco Pedraza,[‡] Sudarson Sekhar Sinha,[†] Avijit Pramanik,[†] Ashton T Hamme,[†] Zikri Arslan,[†] Dhiraj Sardar,[‡] and Paresh Chandra Ray*[,†]

[†]Department of Chemistry and Biochemistry, Jackson State University, Jackson, Mississippi 39217, United States;

[‡]Department of Physics and Astronomy, University of Texas at San Antonio, San Antonio, Texas 78249, United States

ABSTRACT: More than a billion people lack access to safe drinking water that is free from pathogenic bacteria and toxic metals. The World Health Organization estimates several million people, mostly children, die every year due to the lack of good quality water. Driven by this need, we report the development of PGLa antimicrobial peptide and glutathione conjugated carbon nanotube (CNT) bridged three-dimensional (3D) porous graphene oxide membrane, which can be used for highly efficient disinfection of *Escherichia coli* O157:H7 bacteria and removal of As(III), As(V), and Pb(II) from water. Reported results demonstrate that versatile membrane has the capability to capture and completely disinfect pathogenic pathogenic *E. coli* O157:H7 bacteria from water. Experimentally observed disinfection data indicate that the PGLa attached membrane can dramatically enhance the possibility of destroying pathogenic *E. coli* bacteria via synergistic mechanism. Reported results show that glutathione attached CNT-bridged 3D graphene oxide membrane can be used to remove As(III), As(V), and Pb(II) from water sample at 10 ppm level. Our data demonstrated that PGLa and glutathione attached membrane has the capability for high efficient removal of *E. coli* O157:H7 bacteria, As(III), As(V), and Pb(II) simultaneously from Mississippi River water.

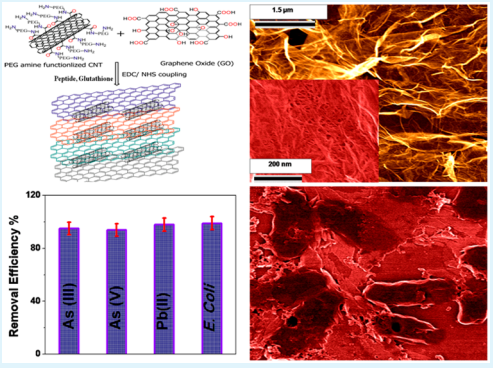

KEYWORDS: *3D porous graphene oxide membrane, CNT-bridged graphene oxide, E. coli O157:H7 bacteria removal, bacteria disinfection, separation of As(III), As(V) and Pb(II) from water*

1. INTRODUCTION

Even in the 21st century, several billion people lack good quality drinking water that is free from pathogenic bacteria and toxic metals.[1−4] According to the World Health Organization (WHO),[3] water contamination by fecal indicator pathogenic bacteria such as *Escherichia coli* O157:H7 kills more than 10 million children/year under the age of five. Current technology to remove pathogenic bacteria from water is mainly chemical treatment.[1,2,5,6] Due to the chemical resistance, several *E. coli* O157:H7 strains have become resistant to common disinfection methods, and thus, a need has arisen for new technologies that can be used for highly effective removal and disinfection of pathogens from water.[1,2,5,6] On the other hand, due to the rapidly growing world population, industrialization, intensification of agricultural activities, and urbanization, society faces a major health risk due to the presence of various toxic heavy metals such as As and Pb in natural waters beyond acceptable limits.[7−13]

According to the World Health Organization (WHO), 180 million people from more than 70 countries have been exposed to toxic levels of arsenic from drinking water.[4] It is well documented that long-time exposure of arsenic can cause skin, liver, lung, and bladder cancers, which have killed more than 40,000 people in Bangladesh in past few years.[4,8] As a result, WHO has established arsenic tolerance level of maximum of 10 μg As/L (10 ppb) in drinking water.[4] Other groundwater contaminant which is highly toxic to human health is Pb(II), which can affect the immune system.[13−15] It is well documented that Pb(II) builds up in the body over the years and damages kidneys, liver, blood, and brain cells.[15] Despite the availability of modern technology such as chemical precipitation, adsorption, membrane filtration, or photocatalytic degradation,[7,8] more than 500 million people are drinking groundwater with As(III), As(V), and Pb(II) concentrations well above the toxicity level. Driven by this need, we report herein the development of peptide conjugated carbon nanotube (CNT) bridged hybrid graphene oxide based three-dimensional (3D) membrane for highly efficient of disinfection of *E. coli* O157:H7 bacteria, as shown in Scheme 1. We have also reported that same membrane can be used for the removal of As(III), As(V), and Pb(II) from water. The novelty of the reported graphene oxide material based technology is based on

Received: June 7, 2015
Accepted: August 14, 2015
Published: August 14, 2015

DOI: 10.1021/acsami.5b05012
ACS Appl. Mater. Interfaces 2015, 7, 19210−19218

Scheme 1. Schematic Representation of the Disinfection of *E. coli* O157:H7 Pathogens and Separation of Toxic Metals Using PGLa and Glutathione-Conjugated CNT-Bridged Porous Graphene Oxide Membrane[a]

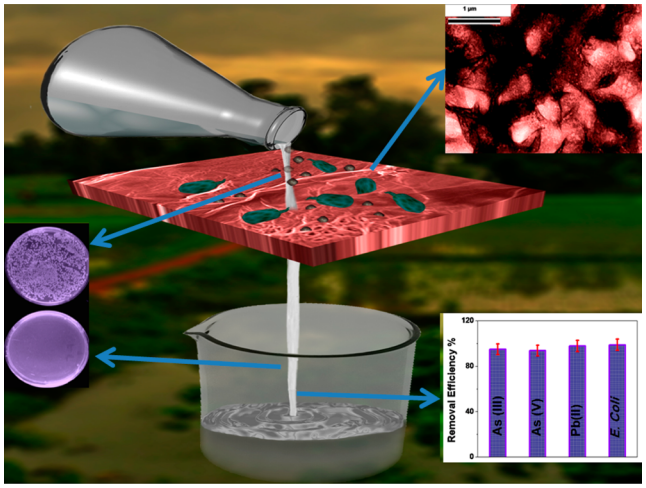

[a](Inset, left) TEM picture of *E. coli* pathogens being captured by 3D membrane. (Inset, top right) Bacteria colony counting results show that no *E. coli* O157:H7 is present in the water once it has been passed through the membrane. (Inset, bottom right) Removal efficiency data shows the membrane cab be used to separate biological and chemical toxin simultaneously.

separation and removal of biological and chemical toxins selectively and simultaneously.

In the past few years, we and other groups have demonstrated that, due to possible large scale production at low cost, high specific surface area, low mass density, and good flexibility, graphene-based membranes with interconnected porous structures possess novel physical and chemical properties.[16−25] Engineered graphene-material-based membranes have demonstrated significant potential for broad use in a variety of water treatment applications.[26−33] Because two-dimensional (2D) graphene oxide (GO) has plenty of hydrophobic basal plane and hydrophilic oxygen-containing groups on the surface,[34−39] we have developed three-dimensional (3D) graphene oxide based membrane via covalent functionalized using one-dimensional (1D) carbon nanotobe (CNT).

In the last two decades, due to unique properties, 1D CNTs have become advanced materials for possible future applications.[40−47] In our synthesis, we used 1D CNTs to physically separate 2D graphene oxide sheets from accumulation and to increase the porous size of the membrane. To capture and kill pathogens, we have developed PGLa antimicrobial peptide conjugated membrane with a pore size of around 400 nm, which not only can capture *E. coli* O157:H7 pathogens from water but also has the capability to kill *E. coli* O157:H7 on contact. PGLa is an α-helical peptide of 21 amino acids ($GMASKAGAIAGKIAKVALKAL\text{-}NH_2$), which is known to destroy bacteria by interacting with their lipid membranes.[48−51] Similarly, for the selective removal of Pb(II) and As(III) from water sample, we have modified the membrane with glutathione. Glutathione (γ-L-glutamyl-L-cysteinyl-glycine) is a tripeptide which exists in the cells and protects cellular membranes from the toxic effects of heavy metals by forming complex with Pb(II), As(III), As(V) etc.[10−15] Our experimental data show that PGLa and glutathione peptide conjugated porous membrane can be used as a versatile membrane to remove pathogens and toxic metals and to kill *E. coli* O157:H7 simultaneously.

2. EXPERIMENTAL SECTION

2.1. Materials. All the chemicals including PGLa, glutathione, single wall carbon nanotube, graphite, poly(ethylene glycol) (PEG), $KMnO_4$, nitric acid, ethylene glycol, arsenic, and lead salts were purchased from Fisher Scientific and Sigma-Aldrich. *E. coli* O157:H7 bacteria and growth media to grow bacteria were purchased from the American Type Culture Collection (ATCC, Rockville, MD).

2.2. Synthesis of Water-Soluble 2D Graphene Oxide. We have synthesized water-soluble 2D graphene oxide using modified Hummers method, as we have reported recently.[21,25] For this purpose, we have performed graphite exfoliation by strong oxidizing agents, as shown in shown in Scheme 2A.[16−25]

In brief, in the first step, 1.8 g of graphite flakes was treated with 1.8 g of $NaNO_3$ in 80 mL of H_2SO_4 and 5g of $KMnO_4$ for 30 min without changing the temperature. After the recation, black paste was obtained. In the next step, we filtered and redispersed the obtained graphene oxide in 150 mL of water and sonicated the mixture for several hours for exfoliation. At the end, water-soluble 2D graphene oxide was obtained. We used ultrahigh resolution field emission scanning electron microscopy (FE-SEM HITACHI) coupled with a BF/DF Duo-STEM detector and energy-dispersive X-ray spectroscopy (EDX; Bruker) to characterize 2D graphene oxide. As shown in Figure 1A, EDX mapping shows the presence of C and O in water-soluble graphene oxide.

2.3. Synthesis of Water-Soluble PEG Amine Functionalized SWCNT. For the development of water-soluble PEG amine functionalized single wall carbon nnaotube (SWCNT), in the initial site, we have performed the oxidative treatments of SWCNT using 3:1 ratio of concentrated sulfuric acid and nitric acid,[40−48] as shown in Scheme 2B. During this process, SWCNT tips were chemically functionalized by carboxy group and water-soluble carboxy functionalized SWCNT was obtained. In the next step, we have functionalized bis amine PEG ($H_2N\text{-}PEG\text{-}NH_2$) with water-soluble SWCNTs by treating the $-CO_2H$ of SWCNT with aimne group of PEG in the presence of EDC cross-linking agent under inert medium. For this development, we have used the coupling chemistry between $-CO_2H$ group of SWCNT and $-NH_2$ group of $H_2N\text{-}PEG\text{-}NH_2$ to develop amine PEG coupled water-soluble SWCNT, a shown in Scheme 2B. At the end, we have used JEOL 2010-F microscope (TEM) for the characterization of water-soluble PEG amine functionalized SWCNT.

2.4. Synthesis of PGLa and Glutathione-Conjugated CNT-Bridged 3D Graphene Oxide Membrane. Oxygen-containing functional groups in water-soluble 2D graphene oxide and amine group in PEG-coupled water-soluble SWCNTs are serve as anchoring points for developing CNT-bridged 3D graphene oxide membrane. For the selective disinfection of *E. coli* bacteria and separation of As(III) and Pb(II), we have developed PGLa and glutathione-conjugated porous membrane. To accomplish this, we used coupling chemistry between $-CO_2H$ group of 2D graphene oxide and $-NH_2$ group of glutathine, PGLa peptide and PEG coupled water-soluble SWCNTs via amide linkages as shown in Scheme 2C. For this purpose, 20 mL of 2D graphene oxide, 20 mL of amine PEG-coupled SWCNT, 100 mg of glutathione, and 80 mg of PGLa peptides were mixed together and sonicated for 10 min. After sonication, samples were kept on oil bath at about 60 °C under a hood for 80 min. At the end, we have obtained PGLa and glutathione-conjugated CNT-bridged 3D graphene oxide semisolid foam, which was used to develop 8 × 8 cm membrane using spin-casting. The membrane structure is shown in Figure 1G. Then, we characterized 3D membrane using scanning electron microscope (SEM), EDX, Fourier transform infrared spectroscopy (FTIR), and Raman spectroscopy. Figure 1C,D display high-resolution SEM image with energy-dispersive X-ray spectroscopy (EDX) mapping of the PGLa peptide and glutathione-conjugated CNT-bridged membranes microstructure, which show an interconnected 3D network with a pore size of 300−500 nm. The inset high-resolution picture in Figure 1C clearly shows the presence of CNT in

DOI: 10.1021/acsami.5b05012
ACS Appl. Mater. Interfaces 2015, 7, 19210−19218

Scheme 2. Schematic Representation Showing (A) the Synthesis Procedure for Graphene Oxide from Graphite, (B) Our Synthesis Procedure to Develop PEG-Amine-Functionalized CNT, and (C) the Synthesis Procedure for the CNT-Bridged 3D Graphene Oxide Membrane

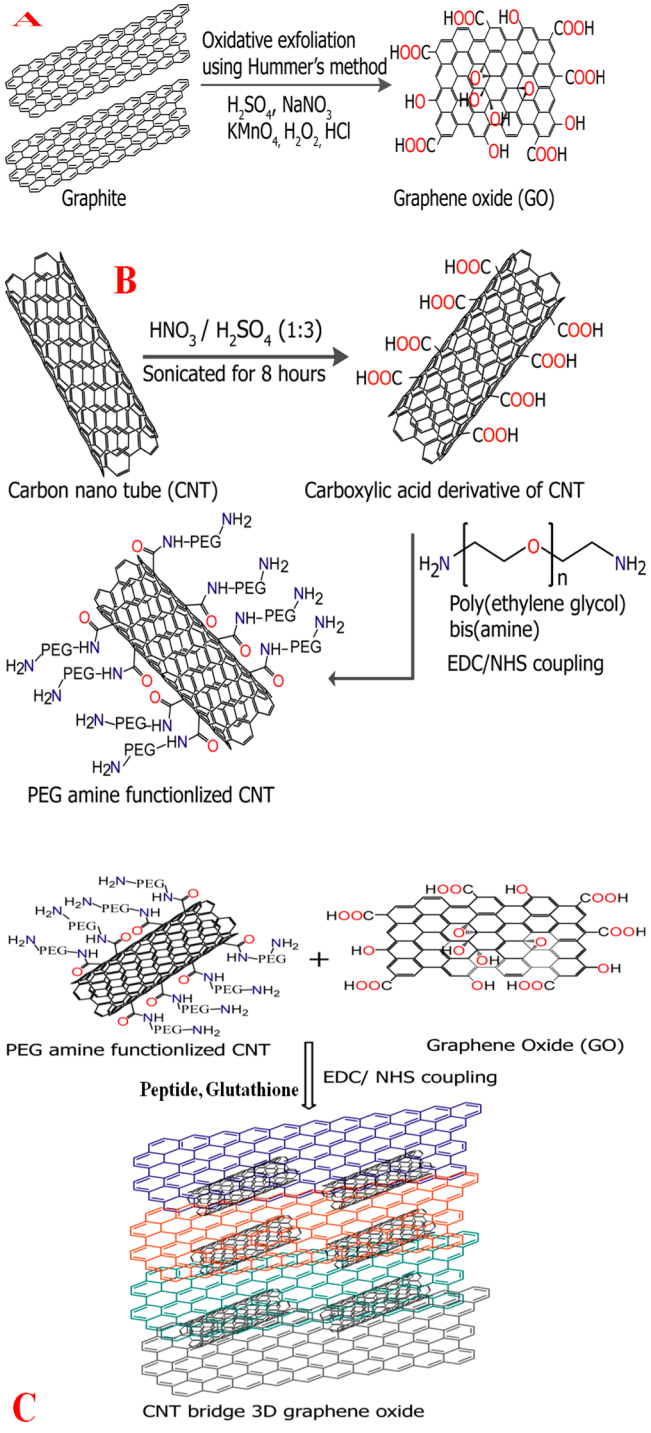

3D membrane. The EDX mapping, as reported in Figure 1D, clearly shows the presence of C, N, S, and O in the 3D hybrid graphene oxide network, which indicates the presence CNT, GO, glutathione and peptides. Next, we have used Thermo Nicolet Nexus 870 FTIR spectrometer equipped with three beam splitters to find out the chemical composition of PGLa peptide and glutathione attached CNT bridges 3D graphene oxide. As shown in the Figure 1E, the FTIR spectrum of the PGLa peptide and glutathione-conjugated CNT-bridged membranes show a very strong band at ~3325 cm^{-1}, which can be attributed as peptide Amide A band. In the reported IR spectra, we have observed an amide I band at ~1750 cm^{-1} which is mainly due to the stretching vibrations of the C═O bond of the amide. We have also observed an amide II band at ~1550 cm^{-1}, which is mainly due to the in-plane NH bending vibration from peptide. Similarly, an amide III band ~1260 cm^{-1} is mainly due to the peptides. Reported IR spectra at Figure 1E also show a strong band at ~3600 cm^{-1}, which is mainly due to the −OH stretching vibration. Similarly, IR peaks were observed at ~1722 cm^{-1} for the carbonyl (−C═O) stretch of carboxylic acid from graphene oxide and CNT. Figure 1F shows the Raman spectra from CNT-bridged graphene oxide membrane which clearly shows the strong D-band ~1345 cm^{-1} and a G-band ~1625 cm^{-1}.[30−40] Experimentally observed Raman spectra show strong D band which indicates that the surface modification extent for graphene oxide and CNT is high.

2.5. Membrane Characterization. Using nitrogen adsorption analysis via the Brunauer−Emmett−Teller (BET) method, we found that the specific surface area for the membranes was 663 m^2 g^{-1}, and the pore volume was 0.560 cm^3 g^{-1}. From BET analysis, we measured the pore size distribution, which shows an average pore diameter of 400 nm. We measured the water flux by collecting the permeate water through the membrane using an electronic balance and calculated water flux of our membrane is 186.3 L m^{-2} h^{-1} bar^{-1}.

2.6. *E. coli* O157:H7 Bacteria Sample Preparation. *E. coli* O157:H7 were purchased from the ATCC and then cultured using ATCC protocol as instructed. In brief, *E. coli* O157:H7 was rehydrated on 8 to 10 mL of Bacto tryptic soy broth (BD) and incubated at 37 °C for 24 h. In the next step, a single colony of *E. coli* O157:H7 from tryptic agar plate was inoculated into 15 mL of tryptic soy broth for 12 h. We diluted the stock solution of bacteria several times to vary the concentration of *E. coli* O157:H7 from 10^2−10^6 CFU (colony forming unit)/mL.

2.7. Fluorescence Imaging of *E. coli* O157:H7 Bacteria. For fluorescence imaging of *E. coli* O157:H7, we used Cy3 attached PGLa peptide. Imaging experiment was performed using Olympus IX71 inverted confocal fluorescence microscope. For imaging purpose, we used 580 nm light as an excitation source. We used SPOT Insight digital camera for fluorescence collection. Olympus DP capture software has been used for data processing.

2.8. Determination of the Percentage of live *E. coli* O157:H7 bacteria. After removal by 3D membrane, we transferred *E. coli* O157:H7 bacteria to colony-countable plates and incubated for 24 h at 37 °C. After that, the colony number for each plate was counted with a colony counter (Bantex, Model 920 A).

3. RESULTS AND DISCUSSION

To understand whether PGLa-conjugated CNT-bridged 3D graphene oxide membranes can be used for the removal of *E. coli* bacteria from infected water, we spiked 3.2 × 10^6 colony-forming units (CFU)/mL of *E. coli* with 100 mL of distilled water. After 110 min of gentle shaking, we used our 3D membrane to filter the *E. coli* infected water sample. In the next step, to find the removal efficiency of *E. coli* bacteria, we performed reverse transcription polymerase chain reaction (RT-PCR) technique,[52,53] as shown in Figure 2A. We also used colony plating technique on LB agar in water sample as shown in Figure 2D,E. Reported experimental data using colony plating technique and RT-PCR clearly show that about 100% *E. coli* were removed by the PGLa conjugated CNT-bridged 3D graphene oxide membrane.

This very high efficient removal of *E. coli* bacteria using the CNT-bridged membrane is due to the fact that the size of *E. coli* bacteria is about 1.5−2 μm, whereas the pore size of the developed CNT-bridged membrane is about 400 nm. Due to the above fact, only water can pass through the porous membrane and *E. coli* bacteria will not able to go through the PGLa attached membrane. To characterize *E. coli* bacteria

DOI: 10.1021/acsami.5b05012
ACS Appl. Mater. Interfaces 2015, 7, 19210−19218

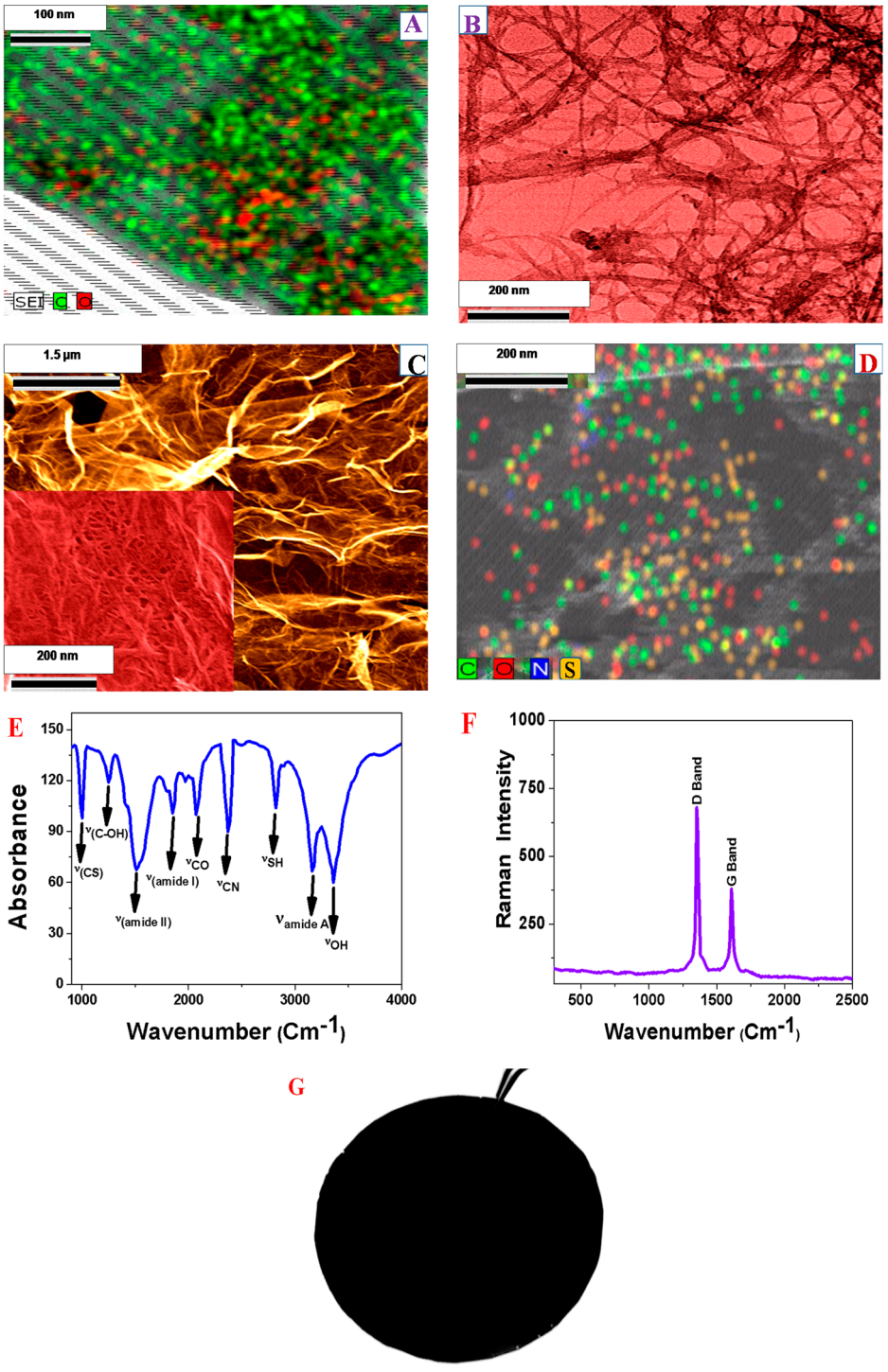

Figure 1. (A) EDX mapping shows the presence of C and O in water-soluble graphene oxide. (B) TEM image of freshly prepared PEG amine functionalized SWCNT. (C) SEM image of PGLa and glutathione-conjugated CNT-bridged graphene oxide membrane shows the 3D structure with pore sizes of 300−500 nm. (D) EDX mapping shows the presence of C, N, S, and O in PGLa and glutathione-conjugated CNT-bridged graphene oxide 3D network membranes. (E) FTIR spectrum shows the existence of amide A, I, and II bands, which indicates the presence of peptides on the 3D membrane. Similarly, the presence of −SH and −CS bands clearly indicate the presence of glutathione on the 3D membrane. The stretches of −CO, −OH, −CN, and −C−OH groups from graphene oxide and CNT can also be seen on the FTIR spectra. (F) Raman spectrum from freshly prepared hybrid membrane clearly indicates the presence of D and G bands in PGLa and glutathione-conjugated CNT-bridged graphene oxide 3D network membranes. (G) Photograph shows freshly prepared PGLa and glutathione-conjugated CNT-bridged porous hybrid graphene oxide membrane.

captured by the membrane, we also used high-resolution TEM, SEM, and fluorescence imaging techniques, as shown in Figures 2B,C,F,G. Reported TEM and SEM images clearly indicate that *E. coli* bacteria are captured on the surface of the membrane. To understand better, we also performed fluorescence imaging as shown in Figures 2F,G. For this purpose, we used Cy3-modified PGLa peptide which was attached with the CNT-bridged 3D membrane. The fluorescence images, as reported in

DOI: 10.1021/acsami.5b05012
ACS Appl. Mater. Interfaces 2015, 7, 19210−19218

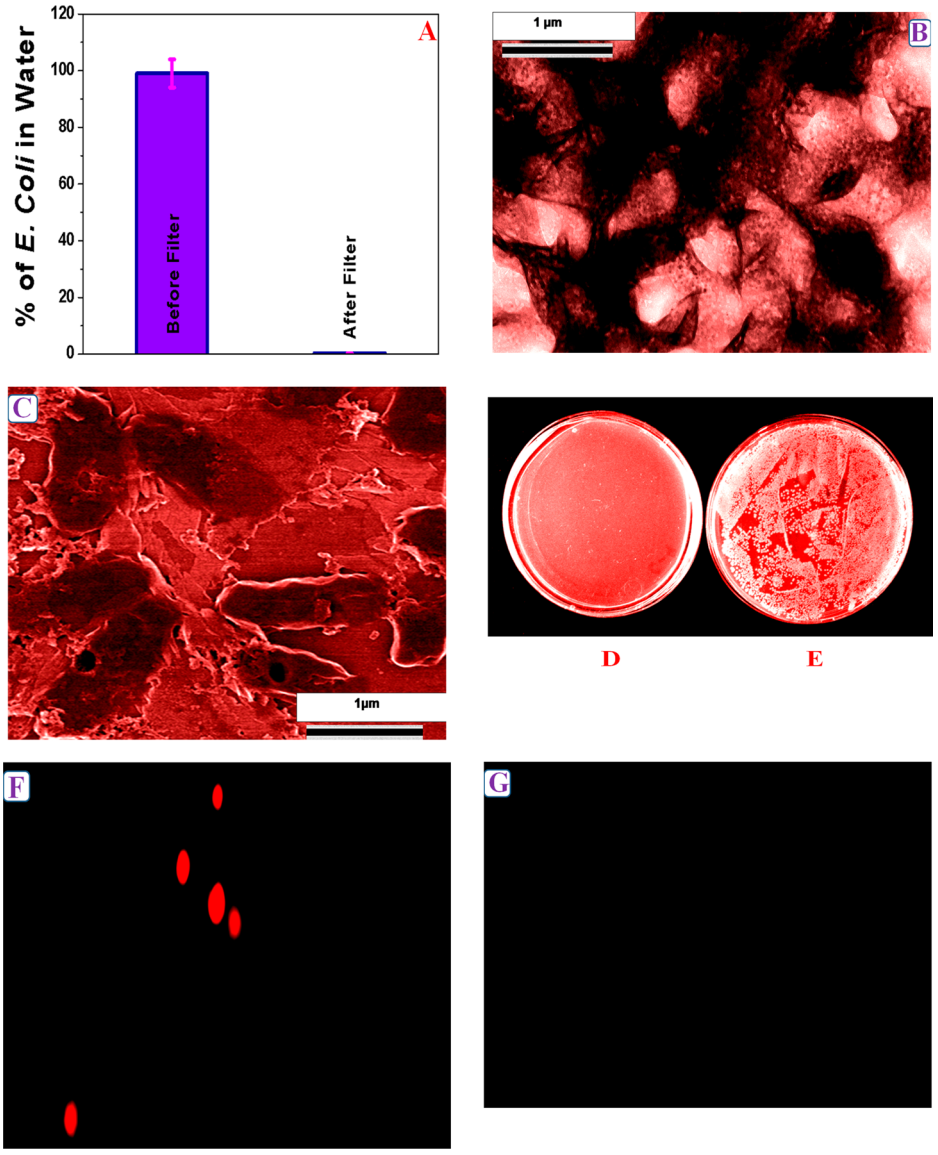

Figure 2. (A) Plot shows *E. coli* O157:H7 removal efficiency using PGLa conjugated CNT-bridged 3D graphene oxide membrane. Reverse transcription polymerase chain reaction (RTPCR) was used to quantify the amount of *E. coli* O157:H7 present. (B) TEM image shows the capture of *E. coli* O157:H7 by CNT-bridged hybrid graphene oxide membrane. (C) SEM image demonstrating the capture of *E. coli* O157:H7 by PGLa-conjugated CNT-bridged 3D graphene oxide based membrane. Colonies of *E. coli* O157:H7 showing the amount of live *E. coli* O157:H7 bacteria (D) after filtration by our membrane and (E) before filtration. (F) Fluorescence image shows the presence of *E. coli* O157:H7 bacteria on membrane after *E. coli* O157:H7 infected water was filtered by membrane. (G) Fluorescence image shows the absence of *E. coli* O157:H7 bacteria in water after separation by membrane.

Figures 2F,G, also confirmed the RT-PCR and colony plating technique results, which clearly indicate that after filtration, *E. coli* bacteria were captured by the membrane and as a result, we have not observed any fluorescence from water sample.

Because *E. coli* O157:H7 is pathogenic and known to be transmitted through contaminated water or by contact, it is very important that the membrane should be able to disinfect *E. coli* O157:H7 bacteria after separation, so that after filtration, the membrane should not be harmful for society. As a result, to understand whether the captured *E. coli* O157:H7 by PGLa conjugated CNT-bridged 3D graphene oxide membranes are alive or dead, we washed the *E. coli* O157:H7 bacteria captured membrane thoroughly using 150 mL of water. After that, we estimated the amount of live *E. coli* O157:H7 bacteria using RT-PCR and colony plating technique. As reported in Figure 3A,B, almost 100% of *E. coli* O157:H7 bacteria were killed when we used PGLa conjugated CNT-bridged 3D graphene oxide membranes.

Next, to find out whether PGLa peptide conjugation is necessary to destroy *E. coli* O157:H7 bacteria, we also performed the same experiment with CNT-bridged 3D graphene oxide membrane in the absence of PGLa antimicrobial peptide attachment. Figure 3A,C clearly shows that most of the *E. coli* O157:H7 bacteria were alive when CNT-bridged 3D graphene oxide membrane was used. The observed very high killing by PGLa peptide attached CNT-bridged membrane can be due to the several facts: It is reported[34−38] that PGLa has the capability to penetrate the outer membrane of bacteria. Due to the insertion of the PGLa into the inner *E. coli* O157:H7 bacteria membrane, lateral expansion of the lipid bilayer occurs. Also, PGLa peptide binding can destabilize the inner membrane of *E. coli* O157:H7 bacteria. Both mechanisms, as discussed

DOI: 10.1021/acsami.5b05012
ACS Appl. Mater. Interfaces 2015, 7, 19210−19218

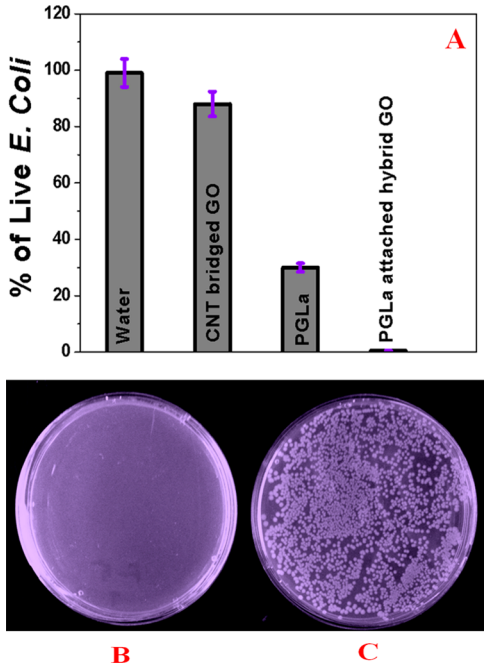

Figure 3. (A) RTPCR data show *E. coli* O157:H7 killing efficiency using CNT-bridged 3D GO without PGLa, with only PGLa, and with PGLa conjugated CNT-bridged 3D graphene oxide membrane. Colonies of *E. coli* O157:H7 bacteria demonstrating the amount of live bacteria after filtration by membrane in the presence of (B) PGLa-conjugated CNT-bridged 3D graphene oxide membrane and (C) CNT-bridged 3D graphene oxide based membrane without PGLa.

above, can be responsible for the *E. coli* O157:H7 bacteria cell death. Another possibility is that 3D graphene oxide can kill *E. coli* O157:H7 bacteria by mechanical wrapping,[33,36,37] as shown in the SEM and TEM images in Figure 2B,C. This mechanical wrapping, as discussed above, may cause induced membrane stress on the *E. coli* O157:H7 membrane by disrupting and damaging cell membranes. The final output can be cell lysis, as reported before.[39−41] Next, to understand how much percentage of *E. coli* O157:H7 bacteria were killed due to the mechanical wrapping, we performed the same experiment by using only CNT-bridged 3D graphene oxide without PGLa peptide. On the other hand, to find out how much *E. coli* O157:H7 bacteria is killed by PGLa peptide, we performed an *E. coli* O157:H7 bacteria killing experiment by adding PGLa directly to the water solution. Figure 3A indicates that PGLa is able to kill roughly 48% of *E. coli* O157:H7 bacteria in the absence of CNT-bridged 3D graphene oxide, whereas CNT-bridged 3D graphene can kill only 11% *E. coli* O157:H7 bacteria. Our experimental data, as reported in Figure 3A, clearly indicate that PGLa attached CNT-bridged 3D graphene oxide membrane exhibit synergistic killing effect, where almost 100% of *E. coli* O157:H7 bacteria were killed. The observed synergistic mechanism can be due to the fact that *E. coli* O157:H7 bacteria are trapped by 3D porus graphene oxide, which causes membrane stress. This condition allows PGLa to bind easily with *E. coli* O157:H7 bacteria and helps to penetrate the outer membrane of bacteria. As a result, *E. coli* O157:H7 bacteria are killed due to the disrupted and damaged cell membranes. So, our reported experimental data clearly show that the multimodal mechanism by PGLa attached CNT-

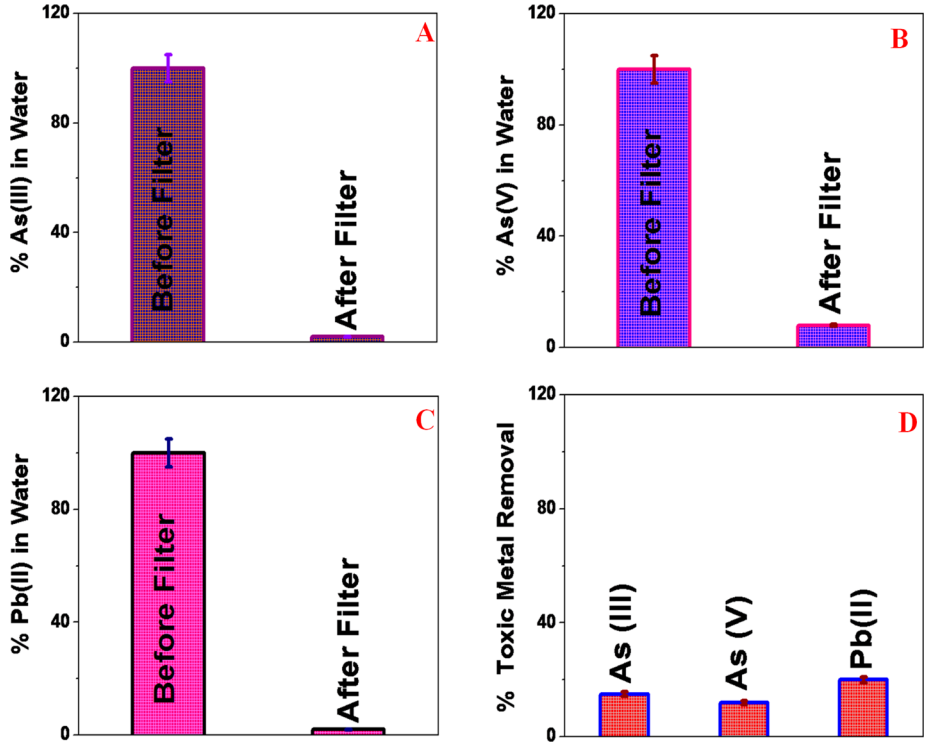

Figure 4. (A) As(III) removal efficiency using glutathione-conjugated CNT-bridged 3D graphene oxide membrane. ICP-MS was used to quantify the amount of As(III) present. (B) As(V) removal efficiency using glutathione-conjugated CNT-bridged 3D graphene oxide membrane. ICP-MS was used to quantify the amount of As(V) present. (C) Pb(II) removal efficiency using glutathione-conjugated CNT-bridged 3D graphene oxide membrane. ICP-MS was used to quantify the amount of Pb(II) present. (D) Percentage of removal efficiency for different toxic metals using CNT-bridged 3D graphene oxide membrane without glutathione. Reported data clearly show that the presence of gluthione is very important for high efficiency As(III), As(V), and Pb(II) removal.

DOI: 10.1021/acsami.5b05012
ACS Appl. Mater. Interfaces 2015, 7, 19210−19218

bridged graphene oxide membrane can dramatically enhance the possibility of destroying *E. coli* O157:H7 bacteria due to the synergistic killing mechanism effect.

Next, to understand whether glutathione-conjugated CNT-bridged 3D graphene oxide membranes can be used for the separation and removal of the As(III) and Pb(II) from water sample, we performed filtration of 100 mL water sample containing 10 ppm As(III), 10 ppm As(V), and 10 ppm Pb(II) using our 3D membrane. We have used inductively coupled plasma mass spectrometry (ICP-MS) for finding the As(III), As(V), and Pb(II) removal amount.

As shown in Figure 4A–C, our data clearly show that more than 96% As(II), 92% As(V), and 98% Pb(II) have been captured by the membrane. This high removal efficiency is due to As (III) and Pb(II) having very high affinity for glutathione, where both metal ions can bind with glutathione via −SH. And for that reason, glutathione is used to protect cellular membranes from the toxic effects of heavy metals. It is also known that glutathione has the capability to reduce As(V) to As(III) and then make a complex with As(III). As a result, a glutathione-attached 3D membrane can remove As(V), As(III), and Pb(II) via the formation of a chemical complex. Another possible mechanism for high removal of toxic metal ions is due to the adsorption by 3D porous graphene oxide. Because the 3D membrane contains an open pore network, which facilitates fast diffusion of As(III), As(V), and Pb(II) inside 3D network, it allows CNT-bridged graphene oxide membrane to be a good adsorbent with high adsorption capacity for the removal of heavy metal ions. Reported heavy metal removal efficiency for multiple toxic metals together is around 20% higher than previously reported efficiency for individual toxic metal.[35,38]

To understand the contribution of each possible mechanism for the very high toxic metals separation efficiency using 3D graphene oxide membrane, we developed a CNT-bridged 3D membrane without glutathione. As shown in Figure 4D, our experimental data clearly show that only 12% of As(III), 9% of As(V), and 18% of Pb(II) can be removed via adsorption mechanism using CNT-bridged 3D graphene oxide membrane. On the other hand, more than 95% of As(III) and Pb(II) removal is possible when glutathione is present. Our reported experimental data clearly show that the presence of glutathione is necessary for very highly efficient removal of toxic metals like As(III), As(V), and Pb(II).

Next, to find out whether our membrane can be used for the separation of pathogens and toxic metals from the environmental sample, we used Mississippi River water spiked with *E. coli*, arsenic, and lead. Because Mississippi River water contains different metal ions, by using river water, we are able to test if our membrane can be used for targeted metal ion separation in the presence of other metal ions. For this purpose, we collected water samples from Mississippi River and spiked 3×10^6 colony-forming units (CFU)/mL of *E. coli* and 10 ppm As(III), 10 ppm As(V), and 10 ppm Pb(II). After that, we performed filtration of 100 mL spiked Mississippi River water sample using our PGLa and glutathione conjugated CNT-bridged 3D membrane. At the end, we have used inductively coupled plasma mass spectrometry (ICP-MS) for finding the As(III), As(V) and Pb(II) removal amount. We have also used RT-PCR to find out the removal efficiency for *E. coli* O157:H7 bacteria. As shown in Figure 5, our data clearly show that PGLa and glutathione conjugated CNT-bridged 3D graphene oxide membrane can be used for the removal of more than 99% of *E. coli* O157:H7 bacteria, 98% of As(III), 94% of As(V), and 98% of Pb(II) simultaneously from infected Mississippi River water.

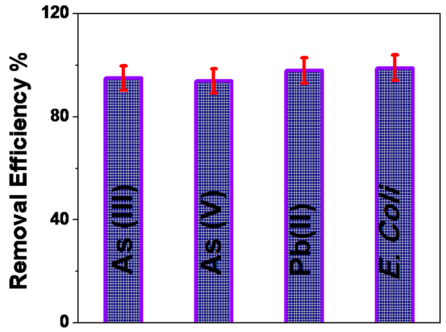

Figure 5. Plot showing percentage of removal efficiency of different toxic metals and *E. coli* bacteria by PGLa and glutathione attached CNT-bridged 3D graphene oxide membrane from Mississippi River water.

4. CONCLUSIONS

In conclusion, we have reported the development of PGLa and glutathione conjugated CNT-bridged 3D graphene oxide membrane for disinfection of pathogenic *E. coli* O157:H7 bacteria and removal of As(III), As(V), and Pb(II) with very high efficiency. We demonstrated that PGLa antimicrobial peptide conjugated CNT-bridged porous 3D graphene oxide membrane has the capability to capture and completely disinfect pathogenic pathogenic *E. coli* O157:H7 bacteria from water. Our reported data indicate that because the pore size of the CNT-bridged membrane (∼400 nm) is much smaller than pathogenic *E. coli* O157:H7 bacteria (∼1.5 μm), only water can pass through the porous membrane, whereas *E. coli* O157:H7 bacteria were captured by the membrane, which had been confirmed by SEM, TEM, and fluorescence images. Using RT-PCR and colony counting data, we have shown that almost 100% of pathogenic *E. coli* O157:H7 bacteria can be captured from the water sample using PGLa peptide conjugated membrane. Our reported disinfection data indicate that the PGLa-attached CNT-bridged graphene oxide membrane can dramatically enhance the possibility of destroying pathogenic *E. coli* O157:H7 bacteria via synergistic effect where CNT-bridged 3D graphene oxide helps to trap *E. coli* and allow PGLa to bind easily with *E. coli* O157:H7 bacteria. This helps PGLa to penetrate the outer membrane of bacteria and kill *E. coli* O157:H7 bacteria.

Our experimental results show that glutathione-attached CNT-bridged 3D graphene oxide membrane can be used to remove As(III), As(V), and Pb(II) from water samples at the 10 ppm level. We have shown that the most efficient way to remove toxic metals is to use a glutathione-attached membrane, where glutathione binds with As(III), As(V), and Pb(II) and removes them from water. Our data demonstrate that PGLa and glutathione-attached CNT-bridged 3D graphene oxide membrane has the capability for highly efficient and simultaneous removal of *E. coli* O157:H7 bacteria, As(III), As(V), and Pb(II) from Mississippi River water. Though we are in a relatively early stage of development, our experimental data reported here open up a new possibility for effective removal of pathogenic bacteria and toxic metals from environmental samples. Before the membrane can be used for society, vigorous research needs to be conducted to find a cost-effective

DOI: 10.1021/acsami.5b05012
ACS Appl. Mater. Interfaces 2015, 7, 19210−19218

process for large-scale development and methods to improve the long-term performance.

AUTHOR INFORMATION

Corresponding Author

*E-mail:paresh.c.ray@jsums.edu. Fax: +16019793674.

Notes

The authors declare no competing financial interest.

ACKNOWLEDGMENTS

P.C.R. thanks NSF-PREM (grant no. DMR-1205194) and NIH RCMI (grant no. G12MD0007581) for their generous funding. F.P. thanks NIH RCMI (grant no. G12 MD007591) for his fellowship.

REFERENCES

(1) Drinking Water Chlorination: A Review of Disinfection Practices and Issues. http://www.waterandhealth.org/drinkingwater/wp.html, date of access 03/12/2015.

(2) Billions affected daily by water and sanitation crisis. http://water.org/water-crisis/one-billion-affected/, date of access 03/12/2015.

(3) Health through safe drinking water and basic sanitation. http://www.who.int/water_sanitation_health/mdg1/en/, date of access 03/12/2015.

(4) Health Topics: Arsenic. http://www.who.int/topics/arsenic/en/, date of access 03/12/2015.

(5) Pal, S.; Joardar, J.; Song, J. Removal of E. coli from Water Using Surface-Modified Activated Carbon Filter Media and Its Performance over an Extended Use. *Environ. Sci. Technol.* **2006**, *40*, 6091−6097.

(6) Deng, D.; Zhang, N.; Mustapha, A.; Xu, D.; Wuliji, T.; Farley, M.; Yang, J.; Hua, B.; Liu, F.; Zheng, G. Differentiating Enteric Escherichia coli from Environmental Bacteria Through the Putative Glucosyltransferase Gene. *Water Res.* **2014**, *61*, 224−231.

(7) Fu, F. L.; Wang, Q. J. Removal of Heavy Metal Ions From Wastewaters: A review. *J. Environ. Manage.* **2011**, *92*, 407−418.

(8) Chakraborti, D.; Rahman, M. M.; Das, B.; Murrill, M.; Dey, S.; Mukherjee, S. C.; Dhar, R. K.; Biswas, B. K.; Chowdhury, U. K.; Roy, S. Status of Groundwater Arsenic Contamination in Bangladesh: A 14-year Study Report. *Water Res.* **2010**, *44*, 5789−5802.

(9) Scott, N.; Hatlelid, K. M.; MacKenzie, N. E.; Carter, D. E. Reactions of Arsenic(III) and Arsenic(V) Species with Glutathione. *Chem. Res. Toxicol.* **1993**, *6* (10), 102−106.

(10) Spuches, A. M.; Kruszyna, H. G.; Rich, A. M.; Wilcox, D. E. Thermodynamics of the As(III)−Thiol Interaction: Arsenite and Monomethylarsenite Complexes with Glutathione, Dihydrolipoic Acid, and other Thiol Ligands. *Inorg. Chem.* **2005**, *44*, 2964−2972.

(11) Shen, S. W.; Li, X. F.; Cullen, W. R.; Weinfeld, M.; Le, X. C. Arsenic Binding to Proteins. *Chem. Rev.* **2013**, *113*, 7769−7792.

(12) Kalluri, J. R.; Arbneshi, T.; Khan, S. A.; Neely, A.; Candice, P.; Varisli, B. M.; Washington, M. S.; Robinson, B.; Banerjee, S.; Singh, A. K.; Senapati, D.; Ray, P. C. Use of Gold Nanoparticles in a Simple Colorimetric and Ultrasensitive Dynamic Light Scattering Assay: Selective Detection of Arsenic in Groundwater. *Angew. Chem., Int. Ed.* **2009**, *48*, 9668−9671.

(13) Mah, V.; Jalilehvand, F. Lead(II) Complex Formation with Glutathione. *Inorg. Chem.* **2012**, *51*, 6285−6298.

(14) Chai, F.; Wang, C. A.; Wang, T. T.; Li, L.; Su, Z. M. Colorimetric Detection of Pb2+ Using Glutathione Functionalized Gold Nanoparticles. *ACS Appl. Mater. Interfaces* **2010**, *2*, 1466−1470.

(15) Beqa, L.; Singh, A. K.; Khan, S. A.; Senapati, D.; Arumugam, S. R.; Ray, P. C. Gold Nanoparticle-Based Simple Colorimetric and Ultrasensitive Dynamic Light Scattering Assay for the Selective Detection of Pb(II) from Paints, Plastics, and Water Samples. *ACS Appl. Mater. Interfaces* **2011**, *3*, 668−673.

(16) Geim, A. K.; Novoselov, K. S. The Rise of Graphene. *Nat. Mater.* **2007**, *6*, 183−191.

(17) Li, X.; Wang, X.; Zhang, L.; Lee, S.; Dai, H. Chemically Derived, Ultrasmooth Graphene Nanoribbon Semiconductors. *Science* **2008**, *319*, 1229−1232.

(18) Gao, W.; Alemany, L. B.; Ci, L.; Ajayan, P. M. New Insights into the Structure and Reduction of Graphite Oxide. *Nat. Chem.* **2009**, *1*, 403−408.

(19) Sun, P.; Zheng, F.; Zhu, M.; Song, Z.; Wang, K.; Zhong, M.; Wu, D.; Little, R. B.; Xu, Z.; Zhu, H. Selective Trans-membrane Transport of Alkali and Alkaline Earth Cations Through Graphene Oxide Membranes Based on Cation-π Interactions. *ACS Nano* **2014**, *8*, 850−859.

(20) Mi, B. Graphene Oxide Membranes for Ionic and Molecular Sieving. *Science* **2014**, *343*, 740−742.

(21) Viraka Nellore, B. P.; Kanchanapally, R.; Pramanik, A.; Sinha, S. S.; Chavva, S. R.; Hamme, A.; Ray, P. C. Aptamer-Conjugated Graphene Oxide Membranes for Highly Efficient Capture and Accurate Identification of Multiple Types of Circulating Tumor Cells. *Bioconjugate Chem.* **2015**, *26*, 235−242.

(22) Sun, P.; Zheng, F.; Zhu, M.; Song, Z.; Wang, K.; Zhong, M.; Wu, D.; Little, R. B.; Xu, Z.; Zhu, H. Selective Trans-Membrane Transport of Alkali and Alkaline Earth Cations through Graphene Oxide Membranes Based on Cation-π Interactions. *ACS Nano* **2014**, *8*, 850−859.

(23) Nair, N. N.; Wu, H. A.; Jayaram, P. N.; Grigorieva, I. V.; Geim, A. K. Unimpeded Permeation of Water Through Helium-Leak-Tight Graphene-Based Membraness. *Science* **2012**, *335*, 442−444.

(24) Han, Y.; Xu, Z.; Gao, C. Ultrathin Graphene Nanofiltration Membrane for Water Purification. *Adv. Funct. Mater.* **2013**, *23*, 3693−3700.

(25) Fan, Z.; Yust, B.; Nellore, B. O. V; Sinha, S. S.; Kanchanapally, R.; Crouch, R. A.; Pramanik, A.; Reddy, S. C.; Sardar, D.; Ray, P. C. Accurate Identification and Selective Removal of Rotavirus Using a Plasmonic−Magnetic 3D Graphene Oxide Architecture. *J. Phys. Chem. Lett.* **2014**, *5*, 3216−3221.

(26) Li, H.; Song, Z.; Zhang, X.; Huang, Y.; Li, S.; Mao, Y.; Ploehn, H. J.; Bao, Y.; Yu, M. Ultrathin, Molecular-Sieving Graphene Oxide Membraness for Selective Hydrogen Separation. *Science* **2013**, *342*, 95−98.

(27) Joshi, R. K.; Carbone, P.; Wang, F. C.; Kravets, V. G.; Su, Y.; Grigorieva, I. V.; Wu, H. A.; Geim, A. K.; Nair, R. R. Precise and Ultrafast Molecular Sieving through Graphene Oxide Membraness. *Science* **2014**, *343*, 752−754.

(28) Kim, H. W.; Yoon, H. W.; Yoon, S. M.; Yoo, B. M.; Ahn, B. K.; Cho, Y. H.; Shin, H. J.; Yang, H.; Paik, U.; Kwon, S. Selective Gas Transport Through Few-Layered Graphene and Graphene Oxide Membraness. *Science* **2013**, *342*, 91−95.

(29) Ghosh, T.; Biswas, C.; Oh, J.; Arabale, G.; Hwang, T.; Luong, N. D.; Jin, M.; Lee, Y. H.; Nam, J. D. Solution-Processed Graphite Membrane from Reassembled Graphene Oxide. *Chem. Mater.* **2012**, *24*, 594−599.

(30) Zhao, G.; Jiang, L.; He, Y.; Li, J.; Dong, H.; Wang, X.; Hu, W. Sulfonated Graphene for Persistent Aromatic Pollutant Management. *Adv. Mater.* **2011**, *23*, 3959−3963.

(31) Zhang, Y.; Tang, Z.-R.; Fu, X.; Xu, Y.-J. TiO_2−Graphene Nanocomposites for Gas-phase Photocatalytic Degradation of Volatile Aromatic Pollutant: Is TiO_2−Graphene Truly Different from other TiO_2−Carbon Composite Materials? *ACS Nano* **2010**, *4*, 7303−7314.

(32) Koenig, S. P.; Wang, L.; Pellegrino, J.; Bunch, J. S. Selective Molecular Sieving through Porous Graphene. *Nat. Nanotechnol.* **2012**, *7*, 728−732.

(33) Kanchanapally, R.; Viraka Nellore, B. P.; Sinha, S. S.; Pedraza, F.; Jones, S. J.; Pramanik, A.; Chavva, S. R.; Tchounwou, C.; Shi, Y.; Vangara, A.; Sardar, D.; Ray, P. C. Antimicrobial Peptide-Conjugated Graphene Oxide Membrane for Efficient Removal and Effective Killing of Multiple Drug Resistant Bacteria. *RSC Adv.* **2015**, *5*, 18881−18887.

(34) Wei, N.; Peng, X.; Xu, Z. Understanding Water Permeation in Graphene Oxide Membranes. *ACS Appl. Mater. Interfaces* **2014**, *6*, 5877−5883.

DOI: 10.1021/acsami.5b05012
ACS Appl. Mater. Interfaces 2015, 7, 19210−19218

(35) Vadahanambi, S.; Lee, S. H.; Kim, W. J.; Oh, I. K. Arsenic Removal from Contaminated Water Using Three-Dimensional Graphene-Carbon Nanotube-Iron Oxide Nanostructures. *Environ. Sci. Technol.* **2013**, *47*, 10510−10517.
(36) Tian, T. F.; Shi, X. Z.; Cheng, L.; Luo, Y. C.; Dong, Z. L.; Gong, H.; Xu, L. G.; Zhong, Z. T.; Peng, R.; Liu, Z. Graphene-Based Nanocomposite as an Effective, Multifunctional, and Recyclable Antibacterial Agent. *ACS Appl. Mater. Interfaces* **2014**, *6*, 8542−8548.
(37) Hu, W.; Peng, C.; Luo, W.; Lv, M.; Li, X.; Li, D.; Huang, Q.; Fan, C. Graphene-Based Antibacterial Paper. *ACS Nano* **2010**, *4*, 4317−4323.
(38) Madadrang, C. J.; Kim, H. Y.; Gao, G. H.; Wang, N.; Zhu, J.; Feng, H.; Gorring, M.; Kasner, M. L.; Hou, S. F. Adsorption Behavior of EDTA-Graphene Oxide for Pb(II) Removal. *ACS Appl. Mater. Interfaces* **2012**, *4*, 1186−1193.
(39) Kumar, S.; Nair, R. R.; Pillai, P. B.; Gupta, S. N.; Lyengar, M. A. R.; Sood, A. K. Graphene Oxide-$MnFe_2O_4$ Magnetic Nanohybrids for Efficient Removal of Lead and Arsenic from Water. *ACS Appl. Mater. Interfaces* **2014**, *6*, 17426−17436.
(40) De Volder, M. F. L.; Tawfick, S. H.; Baughman, R. H.; Hart, A. J. Carbon Nanotubes: Present and Future Commercial Applications. *Science* **2013**, *339*, 535−539.
(41) Hu, L. B.; Hecht, D. S.; Grüner, G. Carbon Nanotube Thin Films: Fabrication, Properties, and Applications. *Chem. Rev.* **2010**, *110*, 5790−5844.
(42) Schnorr, J. M.; Swager, T. M. Emerging Applications of Carbon Nanotubes. *Chem. Mater.* **2011**, *23*, 646−657.
(43) Beqa, L.; Fan, Z.; Singh, A. K.; Senapati, D.; Ray, P. C. Gold Nano-Popcorn Attached SWCNT Hybrid Nanomaterial for Targeted Diagnosis and Photothermal Therapy of Human Breast Cancer Cells. *ACS Appl. Mater. Interfaces* **2011**, *3*, 3316−3324.
(44) Tung, V. C.; Chen, L. M.; Allen, M. J.; Wassei, J. K.; Nelson, K.; Kaner, R. B.; Yang, Y. Low-Temperature Solution Processing of Graphene−Carbon Nanotube Hybrid Materials for High-Performance Transparent Conductors. *Nano Lett.* **2009**, *9*, 1949−1955.
(45) Huang, J. H.; Fang, J.-H.; Liu, C.-C.; Chu, C.-W. Effective Work Function Modulation of Graphene/Carbon Nanotube Composite Films As Transparent Cathodes for Organic Optoelectronics. *ACS Nano* **2011**, *5*, 6262−627.
(46) Cheng, Y. W.; Lu, S. T.; Zhang, H. B.; Varanasi, V.; Liu, J. Synergistic Effects from Graphene and Carbon Nanotubes Enable Flexible and Robust Electrodes for High-Performance Supercapacitors. *Nano Lett.* **2012**, *12*, 4206−4211.
(47) Chen, P.; Xiao, T. Y.; Qian, Y. H.; Li, S. S.; Yu, S. H. A Nitrogen-Doped Graphene/Carbon Nanotube Nanocomposite with Synergistically Enhanced Electrochemical Activity. *Adv. Mater.* **2013**, *25*, 3192−3196.
(48) Tu, Y.; Lv, M.; Xiu, P.; Huynh, T.; Zhang, M.; Castelli, M.; Liu, Z.; Huang, Q.; Fan, C.; Fang, H. Destructive Extraction of Phospholipids from Escherichia coli Membranes by Graphene Nanosheets. *Nat. Nanotechnol.* **2013**, *8*, 594−601.
(49) Melo, M. N.; Ferre, R.; Castanho, M. A. R. B. Antimicrobial Peptides: Linking Partition, Activity and High Membrane-bound Concentrations. *Nat. Rev. Microbiol.* **2009**, *7*, 245−250.
(50) da Silva, A., Jr.; Teschke, O. Effects of the Antimicrobial Peptide PGLa on Live *Escherichia coli*. *Biochim. Biophys. Acta, Mol. Cell Res.* **2003**, *1643*, 95−103.
(51) Nishida, M.; Imura, Y.; Yamamoto, M.; Kobayashi, S.; Yano, Y.; Matsuzaki, K. Interaction of a Magainin-PGLa Hybrid Peptide With Membranes: Insight Into the Mechanism of Synergism. *Biochemistry* **2007**, *46*, 14284−14290.
(52) Jothikumar, N.; Griffiths, M. W. Rapid Detection of Escherichia coli O157:H7 with Multiplex Real-Time PCR Assays. *Appl. Environ. Microbiol.* **2002**, *68*, 3169−3171.
(53) Ibekwe, A. M.; Watt, P. M.; Grieve, C. M.; Sharma, V. K.; Lyons, S. R. Multiplex Fluorogenic Real-Time PCR for Detection and Quantification of *Escherichia coli* O157:H7 in Dairy Wastewater Wetlands. *Appl. Environ. Microbiol.* **2002**, *68*, 4853−4862.

DOI: 10.1021/acsami.5b05012
ACS Appl. Mater. Interfaces 2015, 7, 19210−19218